UC Irvine
UC Irvine Previously Published Works

Title

Air quality impacts of distributed power generation in the South Coast Air Basin of California 2: Model uncertainty and sensitivity analysis

Permalink

https://escholarship.org/uc/item/3tp100r1

Journal

Atmospheric Environment, 41(27)

ISSN

1352-2310

Authors

Rodriguez, MA
Brouwer, J
Samuelsen, GS
et al.

Publication Date

2007-09-01

DOI

10.1016/j.atmosenv.2007.02.049

Copyright Information

Peer reviewed

ELSEVIER

ATMOSPHERIC
ENVIRONMENT

Air quality impacts of distributed power generation in the South Coast Air Basin of California 2: Model uncertainty and sensitivity analysis

M.A. Rodriguez, J. Brouwer, G.S. Samuelsen, D. Dabdub*

Department of Mechanical and Aerospace Engineering, Henry Samueli School of Engineering, 4200 Engineering Gateway Building, University of California Irvine, Irvine, CA 92697, USA

Abstract

Uncertainty and sensitivity of ozone and $PM_{2.5}$ aerosol to variations in selected input parameters are investigated with a Monte Carlo methodology using a three-dimensional air quality model. The selection of input parameters is based on their potential to affect concentration levels of ozone and $PM_{2.5}$ predicted by the model and to reflect changes in emissions due to the implementation of distributed generation (DG) in the South Coast Air Basin (SoCAB) of California. Numerical simulations are performed with the CIT air quality model. Response of the CIT predictions to the variation of selected input parameters is investigated to separate the potential air quality impacts of DG from model uncertainty. This study provides a measure of the model errors for selected species concentrations. A spatial sensitivity analysis is used to investigate the effect of placing DG in specific regions of the SoCAB. In general, results show that confidence in the model results is greatest in locations where ozone and $PM_{2.5}$ concentrations are the highest. Changes no greater than 80% in the nominal values of selected input variables, cause changes of 18% in ozone mixing ratios and 25% for $PM_{2.5}$ aerosol concentrations. Sensitivity analysis reveals that nitrogen oxides (NO_x) emissions and side boundary conditions of volatile organic compounds (VOC) are the major contributors to uncertainty and sensitivity of ozone predictions. An increase in NO_x emissions leads to reductions in ozone mixing ratios at peak times and sites where the maximum values are located. $PM_{2.5}$ aerosol is most sensitive to changes in NH_3 and NO_x emissions. Increasing these emissions leads to higher aerosol concentrations. Sensitivity analyses show that the impacts of DG implementation are highly dependent on both space and time. In particular, ozone concentrations are reduced during the nighttime nearby locations where DGs are installed. However, during the daytime ozone concentrations increase downwind from the sources. A major finding of this study is that the emissions of DG installed in coastal areas produce a significant impact on the production of ozone and $PM_{2.5}$ aerosol in the eastern regions of the SoCAB.
© 2007 Elsevier Ltd. All rights reserved.

Keywords: Distributed power generation; Uncertainty and sensitivity analysis; Monte Carlo analysis; Spatial sensitivity

1. Introduction

Distributed energy resources (DER) have the potential to provide a considerable portion of the

*Corresponding author. Tel.: +1 949 824 6126; fax: +1 949 824 8585.

E-mail address: ddabdub@uci.edu (D. Dabdub).

increased power demands in California and else-where. California is one of the first regions in the world to reorganize its electric power industry, becoming one of the first places where widespread adoption of DER is expected. The use of these distributed generation (DG) resources results in multiple stationary power generators spatially distributed throughout an urban basin, whereas new central-generation sources are typically placed outside the basin. DG implementation may result in significantly different emissions profiles with increased and widely dispersed stationary sources. Therefore, it is important to determine any adverse effects on the air quality of urban centers that may result from additional DG pollutant emissions. Rodriguez et al. (2006) examined the impacts of DG implementation on the air quality of the South Coast Air Basin of California (SoCAB). This study, however, left some outstanding questions unanswered. Namely, are the observed impacts greater than the numerical uncertainties of the model? Are those impacts real? How uncertainties in the input variables that represent DG implementation scenarios will affect the model predictions? Which of these variables are responsible for most of the model uncertainty? How will the placement of DG emissions in specific locations throughout the basin affect the model results?

Russell and Dennis (2000) found that numerical predictions of mathematical models are subjected to various sources of uncertainty. For instance, emissions inventories usually represent the largest uncertainties associated with output concentrations in three-dimensional urban models (Griffin et al., 2002a). Different approaches have been used to evaluate the uncertainty of air quality models (Yang et al., 1997; Hanna et al., 1998, 2001; Moore and Londergan, 2001; Hanna and Davis, 2002; Vardoulakis et al., 2002; Hakami et al., 2003; Sax and Isakov, 2003). Also, Monte Carlo analyses have been used extensively in regional-scale gas-phase mechanisms to address uncertainty assessment (Derwent and Hov, 1988; Gao et al., 1996; Phenix et al., 1998; Bergin et al., 1999; Grenfell et al., 1999; Hanna et al., 2001; Vuilleumier et al., 2001).

This manuscript presents the first study in which unique aspects are considered to include the impacts of DG implementation in the uncertainty and sensitivity analysis of a three-dimensional air quality model. This work examines the response of specific air quality model predictions in order to separate the DG air quality impacts from model uncertainties. It also provides a measure of the error bounds for simulated concentrations of ozone and particulate matter less than 2.5 μm (PM$_{2.5}$). However, the most innovative contributions are the characterization of the spatial variation of the model's errors to determine those areas in the SoCAB where the predictions display the largest uncertainties and the systematic development of scenarios for a thorough spatial sensitivity analysis that investigates the effects of placing DG in specific regions of the SoCAB.

2. Description

Sensitivity results presented in this study are based on the baseline emissions inventory described in Rodriguez et al. (2006). A base line scenario is established with this inventory that accounts for the increase in population by the year 2010. Additionally, an improved model is used in the present work. For instance, the current CIT model incorporates the Caltech atmospheric chemistry mechanism (CACM) (Griffin et al., 2002a,b; 2003; Pun et al., 2002), a detailed atmospheric chemical mechanism that explicitly predicts the formation of semi-volatile products with the potential to be constituents of secondary organic aerosol (SOA). The current study is motivated by the potential air quality effects of DG implementation by the year 2010. After performing various model evaluations, statistical analysis methods are used to identify the input parameters with the largest effect on both, concentrations of selected key species and their associated variance. This section describes the chosen statistical sampling, the multiple regression methodology used to estimate the sensitivity coefficients, and the corresponding uncertainty assessment for the simulation conditions established.

2.1. Latin hypercube sampling

Monte Carlo methods examine the changes in the model's output (species mixing ratios) when a pre-selected set of input parameters varies by repeated sampling from an assumed joint probability distribution. The probability distribution of species mixing ratios along with the mean and other relevant statistics are evaluated from each sample of model output. Monte Carlo analyses using simple random sampling yield reasonable estimates for probability distributions if the sample size is large. However, a large number of sampled cases are

computationally expensive when using a complete three-dimensional air quality model. Latin hypercube sampling (LHS) (McCay et al., 1979) is a stratified sampling technique that has been compared extensively with other procedures (McCay et al., 1979; Iman and Conover, 1980; Stein, 1987; Owen, 1992), and has proved to be more efficient than straight Monte Carlo sampling. The LHS technique used in this study has been described in full detail by Rodriguez and Dabdub (2003).

2.2. Multiple linear regression

Model sensitivity to variations on selected input parameters is explored using multiple linear regression analysis (Derwent and Hov, 1988; Gao et al., 1996; Hanna et al., 2001). However, when many input variables are involved, the direct construction of a regression model containing all input variables may not be the most adequate approach. Moreover, only a small number of input variables typically have an impact on the output variable. Thus, stepwise regression (Helton, 1993) is used as an alternative to construct a regression model containing all the input variables. With stepwise regression, a series of models is constructed. Namely, the first regression model contains the single input variable with the largest impact on the output uncertainty. The second regression model contains the two variables with the largest impact, including the variable from the previous model. Additional models in the sequence are defined until subsequent models are unable to increase meaningfully the amount of variation that can be accounted in the output variable. This study reports the results obtained with the last model in the sequence.

2.3. Simulation conditions

The calculation of uncertainties in complex three-dimensional air quality models poses a major challenge in that a large number of computational simulations is required. Additionally, statistical tools are essential to infer a few useful conclusions from the numerous three-dimensional, time-dependent results (modeled concentrations). An important step in the analysis is the selection of input variables that both, have the potential to affect the concentrations predicted by the model, and reflect changes due to the DG implementation. This selection typically includes parameters such as the meteorology, the chemical reaction rates, and the

initial conditions. The implementation of DG, however, will result in very different emissions profiles from those of central generation. Therefore, this study seeks to understand whether changes in the emission inventory similar to those changes induced by DG emissions make a difference, and to what extent this difference is significant in the predictions of the air quality model. It is also important to characterize the temporal and spatial domain-wide differences in model uncertainties. This characterization will distinguish the numerical uncertainties of the model from the simulated air quality impacts of DG.

Table 1 presents the variables considered in this study, the values of their uncertainty ranges, and their assumed probability density functions. Values for the uncertainty ranges are compiled from published studies (Hanna et al., 1998, 2001). Table 1 shows the careful selection to those quantities, such as boundary conditions and emissions, which drive spatial variation and affect the implementation of DG in the basin. The number of parameters is limited to less than 20 for three main reasons. First, this analysis focuses on the input variables that only affect the uncertainties of ozone and particulate matter. Second, the number of input variables is restricted to decrease the computational demands of the analysis. Third, not all chemical reaction rates need to be included since a comprehensive sensitivity and uncertainty analysis of CACM (Rodriguez and Dabdub, 2003) show that only a subset of reactions is the most influential for ozone formation. Moreover, Rodriguez and Dabdub (2003) showed that the reactions in Table 1 are consistently the most important over different VOC:NO_x ratios.

CIT model simulations are the starting point of the Monte Carlo analysis. The results reported here are obtained with 50 computational model runs. The number of simulations is adequate, given the number of input variables (Hanna et al., 1998, 2001). Each model run spans a period of three simulation days (72 h). However, all the results are based on the third day of simulation to lessen the influence of initial conditions. Lagrangian models confirm (Nguyen and Dabdub, 2002) that more than 90% of the initial conditions leave the computational domain by the second day of simulation. Furthermore, direct sensitivity analysis of multidimensional models (Yang et al., 1997) show that ozone peak sensitivity values to initial conditions are 12 times higher on the first day

Table 1
Uncertainty ranges and associated sigmas for the airshed input variables in the Monte Carlo runs

Variable type	Input variable	Range of uncertainty (σ_g log-normal)
Boundary concentrations	1. Top ozone	1.23
	2. Top NO_x	1.73
	3. Top VOC	1.73
	4. Top NH_3	1.73
	5. Side ozone	1.23
	6. Side NO_x	1.73
	7. Side VOC	1.73
	8. Side NH_3	1.73
Emissions rates	9. Domain-wide NO_x	1.41
	10. Domain-wide VOC	1.41
	11. Domain-wide NH_3	1.41
Chemical reactions	12. $NO_2 + h\nu$	1.30
	13. $NO + O_3 \rightarrow NO_2 + O_2$	1.10
	14. $NO_2 + OH + M \rightarrow HNO_3$	1.10
	15. $HCHO + h\nu$	1.40
	16. $Alkenes + OH \rightarrow RO_2$	1.13
	17. $Aldehydes + h\nu$	1.40

compared to values on the second and subsequent days. Once the simulations are performed, the calculation of probability density functions for each output variable provides a way to characterize the uncertainty of predicted species concentrations. Model sensitivity is based on the regression coefficients estimated with multiple linear regression as detailed in the previous section.

3. Model uncertainty

This section examines the uncertainty ranges exhibited by ozone and particulate matter concentrations as the result of changes in selected input values. Both, spatial and temporal variations of model uncertainties are investigated for the SoCAB. Given the large amount of output data produced by the model, a detailed study of the uncertainties time variation is performed for six stations only (Simi Valley, Burbank, Central Los Angeles, Long Beach, Riverside, and San Bernardino). However, results of these sites represent the general aerosol dynamics and trends for ozone throughout the basin. For example, the location at Central Los Angeles experiences particularly intense emissions from automobiles as a hub of the region's freeway system and also exhibits great secondary photochemistry, whereas Riverside with typically high ozone and $PM_{2.5}$ concentrations represents those areas downwind of major emission sources.

3.1. Time

In order to investigate the uncertainty of modeled species as a function of time, the concentration time series are summarized as box plots. These box plots provide an alternative, more efficient display of the multiple distributions that result from the statistical analyses. Fig. 1 shows ozone mixing ratios as a function of time at selected sites in the form of box plots, using the output of all Monte Carlo simulations. In this figure, the endpoints (hinges) of the gray boxes are formed by the lower and upper quartiles of the data, i.e., where the 25th and 75th percentiles lie. The horizontal line within the box represents the median. The bars above and below the box (whiskers) are drawn from each hinge to the most extreme measurement inside the inner fence. The inner fence is equivalent to 1.5 the difference between upper and lower quartiles (inter-quartile range, IQR).

The selection of a norm is essential to determine the error bounds of the species considered. A value of interest is the 1-h maximum concentration, since this norm is of most concern to those interested in complying with regional and national air quality standards (Gipson et al., 1981; Meyar, 1986). Fig. 1 presents the box plots for the selected locations. This figure shows that for each site the particular hour at which the maximum ozone mixing ratio occurs is different. It is apparent from Fig. 1 that sites at Riverside and San Bernardino are located
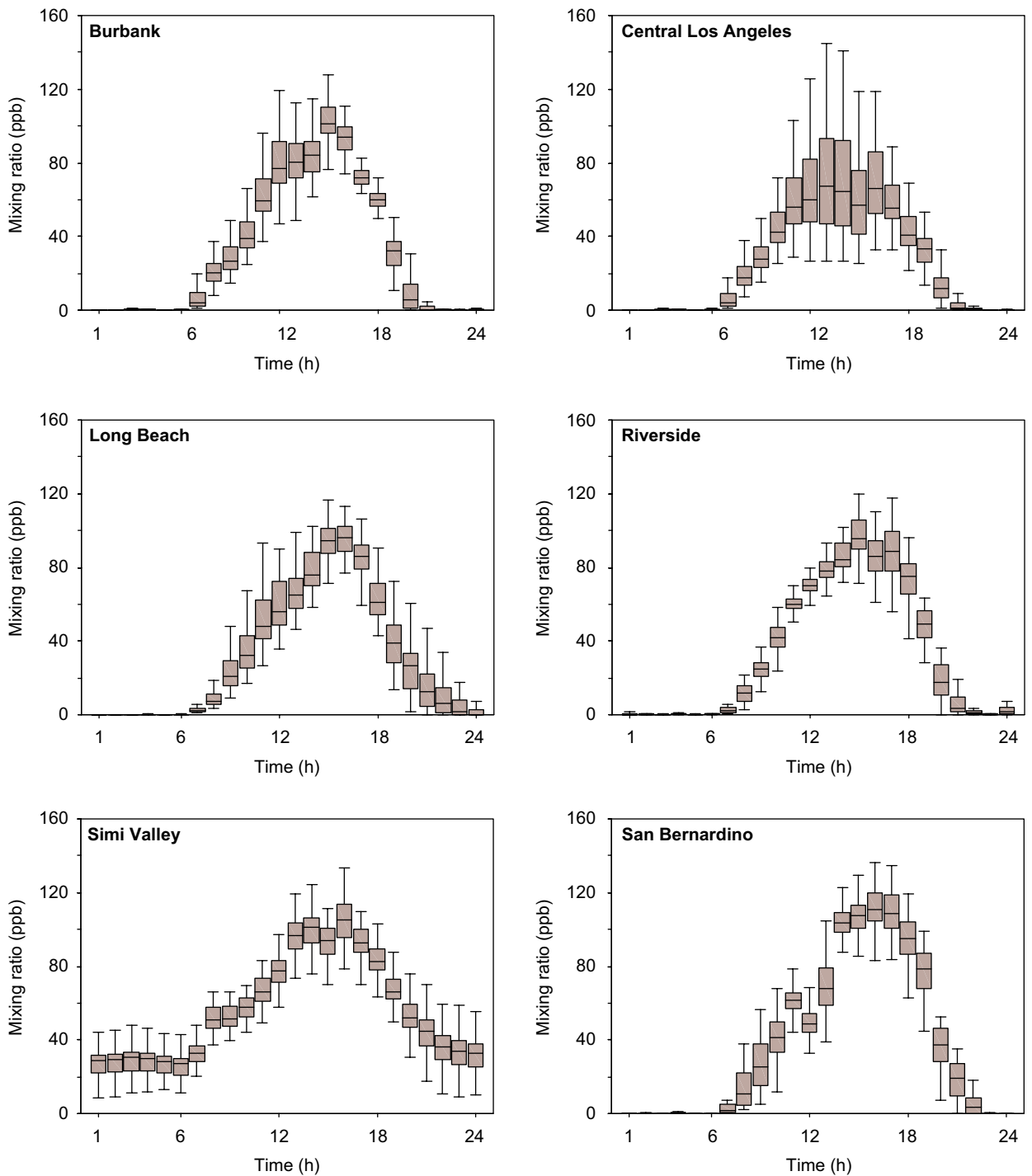
Fig. 1. Box plots for ozone mixing ratios at different sites in the SoCAB. The gray box shows the median, upper and lower quartiles. The ends of the vertical lines indicate the minimum and maximum data values. Results shown for the third day of simulation using the 2010 emissions inventory.

in areas with large domain-wide ozone mixing ratios. Ozone maxima occur at 15:00 in Riverside (median = 96 ppb) and at 16:00 in San Bernardino (median = 111 ppb). The model uncertainty during these peaks is about the same as indicated by the similar IQR values of 15 ppb in both places.

Close examination of the box plots at the peak concentrations shows that the length of the whiskers is approximately the same, an indication that the distribution is symmetrical. This observation suggests that a Gaussian distribution function fits the output data variation adequately and may characterize the uncertainty of these predictions. Fig. 2a compares the cumulative distribution function (CDF) as estimated by the model simulations and the best fit to a normal distribution curve. The comparison is made at Riverside and Central Los Angeles for a 12-h average starting at 8:00. This period comprises most of the daylight time, when ozone concentrations are significant. Similar results (not shown) are observed for the rest of the stations. Two parameters are required to completely determine a normal CDF, namely the mean (μ) and the standard deviation (σ). Fig. 2 shows that calculated

normal distributions fit the data adequately. Furthermore, RMS of the difference between fitted and simulated values when the distributions are assumed normal is always smaller than when the distributions are assumed log-normal. Therefore, a normal probability density distribution is adopted to describe the variance of the predicted concentrations.

Fig. 3 shows the time evolution of $PM_{2.5}$ aerosol at selected sites using box plots. Sites in Riverside and San Bernardino show the largest basin-wide aerosol concentrations, consistent with the formation of secondary particulate matter observed in measurements and previous studies (Meng et al., 1998; Nguyen and Dabdub, 2002). Predicted $PM_{2.5}$ maxima occur at 6:00 and 7:00, respectively, in Riverside (mean = $114\,\mu g\,m^{-3}$) and San Bernardino (mean = $146\,\mu g\,m^{-3}$). Model uncertainty in these
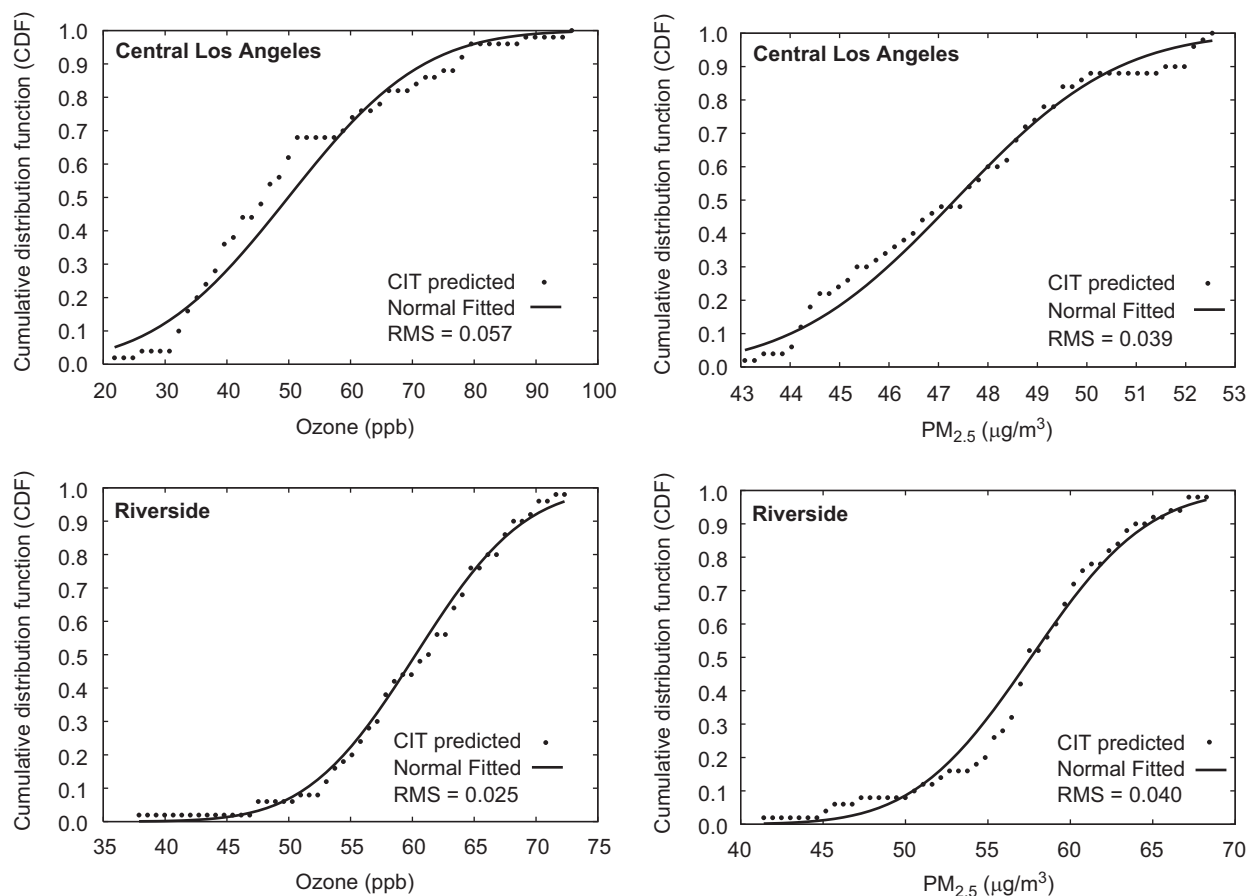

Fig. 2. Comparison between the cumulative distribution function (CDF) estimated with 50 Monte Carlo runs (shown as bullets) and the best-fit normal distribution (solid line). RMS values quantify the differences between estimated and normal CDF fits. Ozone concentrations shown for Riverside at 17:00 and Central Los Angeles at 16:00. $PM_{2.5}$ concentrations shown for Riverside at 07:00 and Central Los Angeles at 06:00. Results shown for the third day of simulation using the 2010 emissions inventory.
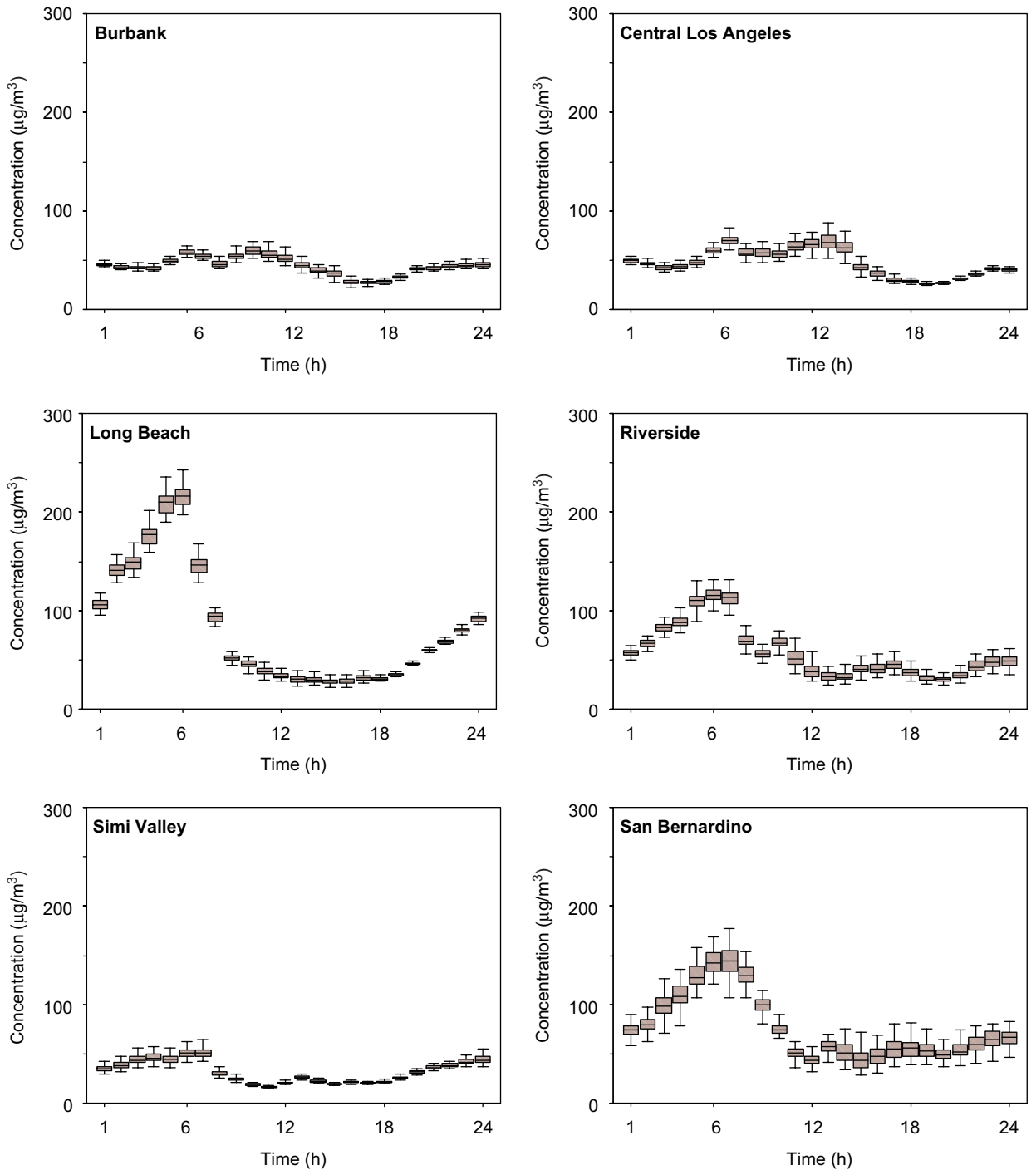
Fig. 3. Box plots for PM$_{2.5}$ concentrations at different sites in the SoCAB. The gray box shows the median, upper and lower quartiles. The ends of the vertical lines indicate the minimum and maximum data values. Results shown for the third day of simulation using the 2010 emissions inventory.

two locations is within the same order of magnitude given the IQR values of 10 and 21 μg m^{-3}, respectively. Fig. 2b compares simulation results

with the fit to a normal CDF. The comparison is made for 24-h average PM$_{2.5}$ aerosol in Riverside and Central Los Angeles. As with ozone, variance

of $PM_{2.5}$ data can also be characterized with a normal probability distribution. The estimated variance is comparable in Riverside ($\sigma = 11\,\mu g\,m^{-3}$) and San Bernardino ($\sigma = 16\,\mu g\,m^{-3}$). As with ozone, the time when the $PM_{2.5}$ uncertainty is the largest does not occur when the predicted $PM_{2.5}$ concentrations reach their maximum.

3.2. Space

The model spatial uncertainties are characterized with probability density distributions that best describe the variance of predicted concentrations in the SoCAB. For ozone, 1-h maximum concentrations are kept for each location in the basin during the 24 h of the last simulation day. This offers a general view of the maximum values everywhere in the domain, regardless of the specific hour when they occurred. For $PM_{2.5}$, a similar process is followed with the exception that concentrations stored represent 24-h averages. Uncertainties associated with

these concentrations are important since compliance with air quality standards is required for domain-wide peak concentrations.

Fig. 4 compares the basin-wide mean, estimated from Monte Carlo simulations, with the ozone base case. The corresponding comparison for aerosol $PM_{2.5}$ is shown in Fig. 5. Base case results in both figures characterize the concentrations calculated using nominal values of the input parameters. These figures show that the location and numerical values of maxima are equivalent for the base case and the mean. Further comparison with calculated median concentrations (not shown) demonstrate that normal probability density distributions describe the variance of predicted concentrations adequately.

Figs. 4 and 5 present the estimated basin-wide standard deviation and mean for ozone and $PM_{2.5}$ concentrations. The eastern side of the basin shows the largest ozone mixing ratios, consistent with previous studies (Meng et al., 1998; Nguyen and Dabdub, 2002) and observations (CARB, 2002,
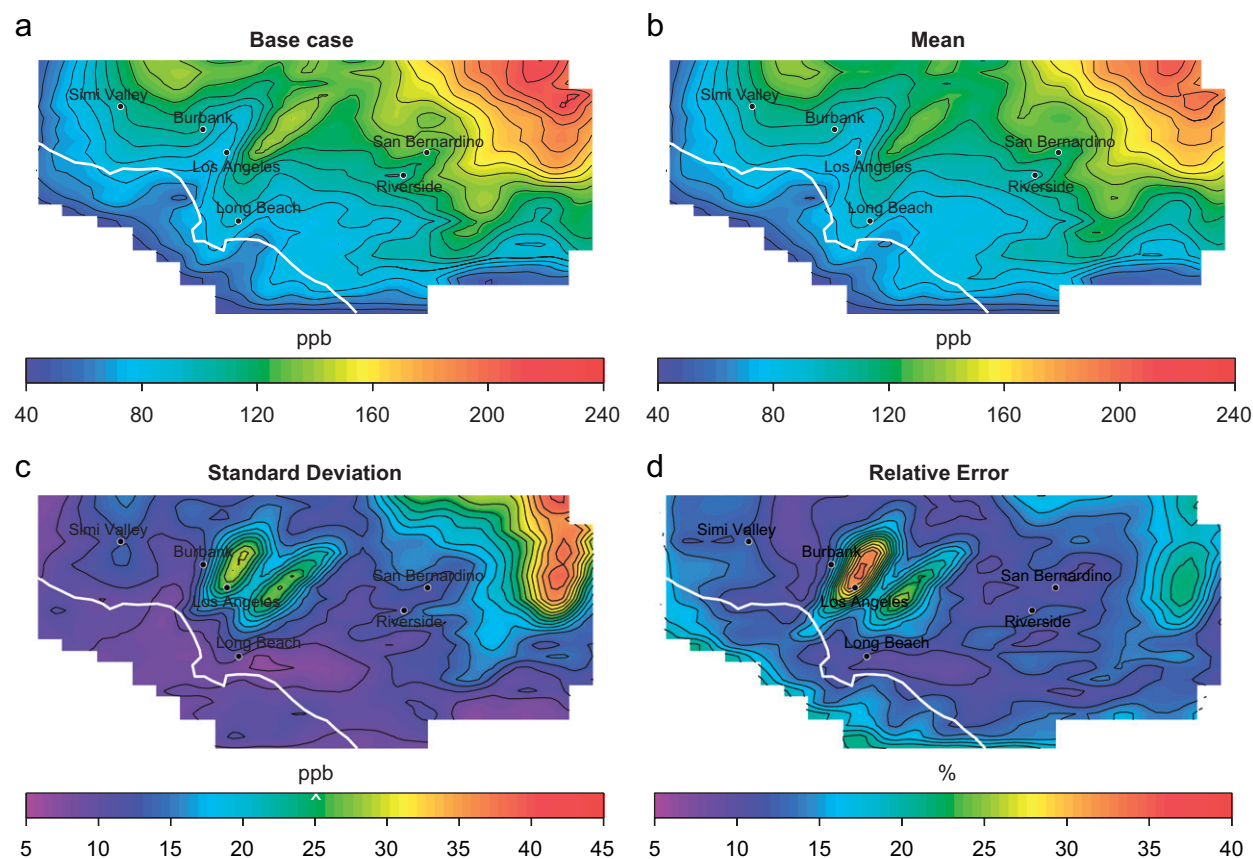

Fig. 4. Plots of ozone in the SoCAB for (a) base case, (b) mean concentrations, (c) standard deviation and (d) estimated relative error for the 1-h maxima of the third day of simulation using the 2010 emissions inventory.
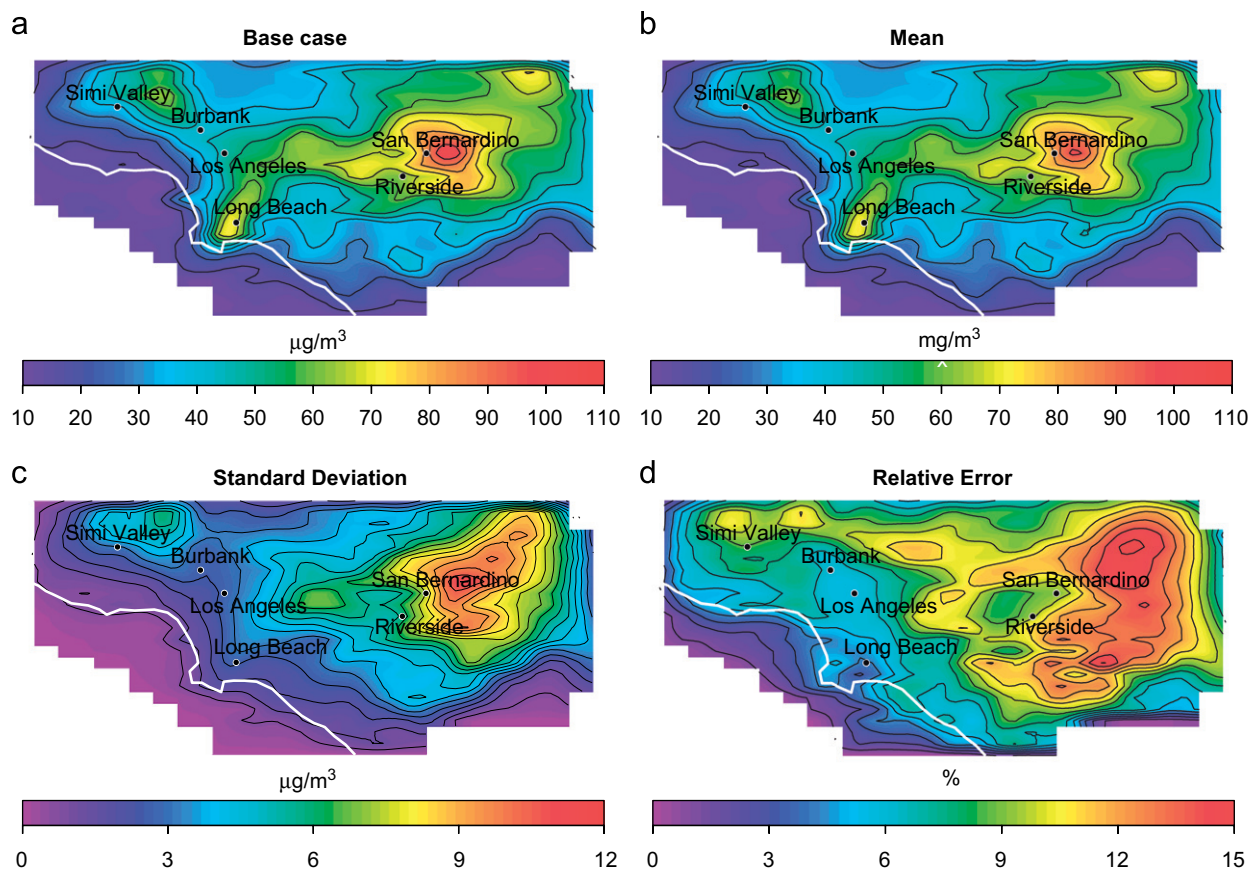
Fig. 5. Plots of $PM_{2.5}$ in the SoCAB for (a) base case, (b) mean concentrations, (c) standard deviation and (d) estimated relative error for the 1-h maxima of the third day of simulation using the 2010 emissions inventory.

2003). Moreover, the calculated σ reveals that the variation of ozone predictions is not the largest in this region of the basin. For instance, the location with the largest mixing ratio (221 ppb) shows a σ of 37 ppb, equivalent to a variance of 17%. In contrast, Central Los Angeles with a large basin-wide variance (42%) exhibits concentrations in the range of 76 ± 32 ppb. The model variance is the result of simultaneous changes in all the input parameters. However, by neglecting the contributions of the emissions and boundary conditions, the model error for ozone predictions decreases significantly. Approximately 8% due to uncertainty in parameters such as the reaction rate constants.

For $PM_{2.5}$ aerosol, Fig. 5 illustrates that the highest concentrations are observed near Riverside and San Bernardino, consistent with previous predictions and observations. East of San Bernardino, the largest domain-wide concentrations ($108 \pm 11 \, \mu g \, m^{-3}$) show a variance of 10%. However, southeast of Riverside, the location with the

largest variance (17%), reaches concentrations of $48 \pm 8 \, \mu g \, m^{-3}$. Although modeled output variations are not the smallest in the regions where $PM_{2.5}$ aerosol reaches its maximum, they are bounded to less than a 15% variance. Again, if the contribution of emissions and boundary conditions are neglected, the estimated model error for $PM_{2.5}$ is reduced substantially. Approximately 6% due to uncertainty in chemical reaction rates.

4. Sensitivity analysis

Sensitivity of ozone and $PM_{2.5}$ aerosol concentrations to selected input variables is explored following the methodology described in Section 2.2. Instead of using stepwise regression analysis at each time step, regression coefficients are calculated using 12-h average concentrations for ozone and 24-h averages for $PM_{2.5}$ aerosol. This approach lessens the computational demands and also provides information of the sensitivity values that are of

interest for compliance with air quality standards. Table 2 presents a list of the input variables with a significant influence in the prediction of ozone mixing ratios at selected sites throughout the domain. Table 2 shows, for each parameter, the calculated standardized regression coefficients (SRC) and the corresponding contribution to the total uncertainty (UC) expressed as a percentage. The regression coefficients values are a measure of the sensitivity of ozone and $PM_{2.5}$ to changes in the input parameters.

In general, the regression model explains 69–98% of the ozone uncertainty as reflected by the R^2 values, with the smallest value (69%) reported for Riverside. Variation in basin-wide NO_x emissions and side boundary conditions imposed on VOC are the most significant contributors to uncertainty and sensitivity of ozone predictions. Ozone boundary conditions have contributions to uncertainty that range from 18.6% to 45.1% in the west side of the SoCAB. The largest contribution (45.1%) is located in Simi Valley, a site close to the boundaries of the computational domain. The SRC sign indicates that increasing NO_x emissions leads to reductions in ozone mixing ratios. In contrast, increasing the values of ozone and VOC's side boundary conditions produces higher ozone mixing ratios.

Results in Table 2 suggest that the regions analyzed are VOC-limited or have low VOC-to-NO_x ratios. This is typical of city centers and plumes immediately downwind of NO_x sources. The results are consistent with the basin being in an overall NO_x-rich state, and with previous findings (Meng et al., 1997). However, most sites also show that VOC and ozone boundary conditions have an important effect on ozone concentrations. Some of these results reflect the proximity to the computational boundaries, like Simi Valley, and the smaller amount of NO_x emission sources in that region (higher VOC-to-NO_x ratios).

A similar analysis is applied to $PM_{2.5}$ for selected sites in the SoCAB (Table 3). The regression model explains 90–95% of the variation that the computational model exhibits for $PM_{2.5}$ aerosol concentrations. In most sites, $PM_{2.5}$ aerosol concentrations are most sensitive to changes in NH_3 and NO_x emissions. The positive sign of the SRC values indicates that any increase in NO_x or NH_3 emissions results in higher $PM_{2.5}$ aerosol concentrations, consistent with the finding that a major component of this aerosol is ammonium nitrate (Nguyen and Dabdub, 2002).

The uncertainty values presented here consider the variation of all input parameters. However, scenarios of DG implementation are formulated by changing emissions only. Results show that when only the contribution to uncertainty from emissions is considered, the current model is sensitive enough to predict air quality impacts of DG emissions as long as changes in peak ozone concentrations are greater than 5 ppb and changes in $PM_{2.5}$ are greater than $13\,\mu g\,m^{-3}$.

5. Spatial sensitivity scenarios

Monte Carlo analyses diagnose the uncertainties of the air quality model to variations in a set of given input parameters. However, there are differences between Monte Carlo and spatial sensitivity analyses. For instance, the Monte Carlo methodology considers changes in the intensity of emissions through multiplicative factors, but their spatial distribution is not modified. This procedure, although necessary, does not explore the spatial sensitivities of emissions and their relevance to predictions. Moreover, the influence of DG installation in the SoCAB needs to be addressed directly. In particular, the type of variations produced by simulation results when DG is placed in specific parts of the basin. To investigate spatial sensitivities, the current section presents a methodology in which only changes to DG emissions added to the baseline are systematically considered.

The development of a set of scenarios to investigate spatial sensitivities is based partly in the general methodology devised by Rodriguez et al. (2006). The total mass emissions selected for this sensitivity study correspond to one of the scenarios with the highest penetration. Namely one in which 20% of the total energy demand by the year 2010 will be supplied by DG. Rodriguez et al. (2006) found this is one scenario with the largest impacts on ozone concentrations due to DG implementation. Instead of using an arbitrary spatial distribution of emissions, five scenarios are developed to separate the adoption of DG by counties in the SoCAB using geographic information systems (GIS) land-use data. In all scenarios, base-loaded emissions are added to the baseline for each county. Specifically, 50 cells of the computational domain are selected using the non-vacant areas provided by the GIS data. This ensures that the emissions variations in all scenarios are equivalent and the simulated effects are not due to a different amount

Table 2
Most important parameters based on the contributions to uncertainty of ozone at selected sites

Riverside			San Bernardino			Los Angeles		
Parameter	SRC[a]	UC[b]	Parameter	SRC	UC	Parameter	SRC	UC
$R^2 = 0.69$			$R^2 = 0.93$			$R^2 = 0.98$		
NO_x emissions	−0.549	29.2	NO_x emissions	−0.755	56.2	NO_x emissions	−0.683	48.3
Side VOC B.C.	0.478	23.7	Side VOC B.C.	0.494	24.8	Side VOC B.C.	0.531	32.9
$NO + O_3$	0.282	8.0	VOC emissions	0.250	6.4	Side O_3 B.C.	0.345	11.7
			$NO + O_3$	0.146	1.9	Side NO_x B.C.	0.199	4.1
			Alkenes + OH	0.120	1.4	VOC emissions	0.059	0.3

Burbank			Long Beach			Simi Valley		
Parameter	SRC	UC	Parameter	SRC	UC	Parameter	SRC	UC
$R^2 = 0.94$			$R^2 = 0.96$			$R^2 = 0.98$		
NO_x emissions	−0.767	60.7	NO_x emissions	−0.674	46.8	Side O_3 B.C.	0.702	45.1
Side O_3 B.C.	0.417	18.6	Side O_3 B.C.	0.518	29.4	Side NO_x B.C.	0.572	28.2
Side NO_x B.C.	0.259	7.7	Side VOC B.C.	0.361	14.3	Side VOC B.C.	−0.369	13.7
Side VOC B.C.	0.234	5.4	Side NO_x B.C.	0.217	4.6	NO_x emissions	0.305	9.4
						VOC emissions	0.062	0.4
						NH_3 emissions	−0.056	0.3

[a]Standardized regression coefficient.
[b]Uncertainty contribution in percentage (%).

Table 3
Most important input parameters based on the contributions to the uncertainty of PM$_{2.5}$ aerosol concentrations at selected sites

Riverside			San Bernardino			Los Angeles		
Parameter	SRC[a]	UC[b]	Parameter	SRC	UC	Parameter	SRC	UC
$R^2 = 0.90$			$R^2 = 0.93$			$R^2 = 0.93$		
NO$_x$ emissions	0.792	61.1	NO$_x$ emissions	0.773	56.6	NH$_3$ emissions	0.723	45.6
NH$_3$ emissions	0.436	18.9	NH$_3$ emissions	0.531	28.3	NO$_x$ emissions	0.476	21.9
Side VOC B.C.	−0.146	2.6	NO + O$_3$	0.174	3.1	Side NO$_x$ B.C.	0.316	10.8
NO + O$_3$	0.131	1.8	Side O$_3$ B.C.	−0.137	1.6	Side O$_3$ B.C.	0.258	7.2
Side O$_3$ B.C.	−0.131	1.5	VOC emissions	0.104	1.0	NO + O$_3$	0.157	2.5
Side NO$_x$ B.C.	−0.122	1.4	NO$_2$ + hv	0.096	0.9	NO$_2$ + hv	0.141	1.9
Alkenes + OH	0.112	1.2				Side VOC B.C.	0.121	1.4
Burbank			Long Beach			Simi Valley		
Parameter	SRC	UC	Parameter	SRC	UC	Parameter	SRC	UC
$R^2 = 0.94$			$R^2 = 0.94$			$R^2 = 0.95$		
NO$_x$ emissions	0.667	38.9	NH$_3$ emissions	0.685	39.1	NO$_x$ emissions	0.701	43.7
NH$_3$ emissions	0.631	36.0	NO$_x$ emissions	0.518	25.4	Side NO$_x$ B.C.	0.539	24.9
Side NO$_x$ B.C.	0.303	8.2	Side NO$_x$ B.C.	0.404	16.4	Side VOC B.C.	−0.425	16.2
Side VOC B.C.	−0.250	5.6	Side O$_3$ B.C.	0.300	9.1	NH$_3$ emissions	0.258	6.1
Side O$_3$ B.C.	0.126	1.6	NO$_2$ + hv	0.136	1.8	Side O$_3$ B.C.	0.128	1.7
NO$_2$ + hv	0.123	1.4	NO + O$_3$	0.098	0.9	NO$_2$ + hv	0.087	0.8
NO + O$_3$	0.111	1.3						

[a]Standardized regression coefficient.
[b]Uncertainty contribution in percentage (%).

of DG implementation in each county. Fig. 6 shows the areas in each county where additional DG emissions are placed.

Fig. 7 shows the difference in 1-h average ozone concentrations between each scenario and the 2010 base-case at the hour when the largest impacts occur. In general ozone impacts range from -36 to $39\,ppb$, which are significant differences compared to the impacts of the high penetration scenario investigated by Rodriguez et al. (2006) ($\pm 8\,ppb$). Furthermore, this illustrates the importance of DG spatial accumulation since both the high penetration and the county scenarios introduce the same amount of emissions mass into the basin. Areas where emissions are typically low, such as Ventura present the largest impacts. Ozone increases with respect to the base-case can be as large as $39\,ppb$. In this region, increases on NO_x emissions reduces ozone formation locally during the nighttime, however, as the sun rises at around 8:00 the differences start to become positive indicating an increase in ozone concentrations. At night NO from DG emissions scavenges ozone. During the day Ventura is in a NO_x-limited region where NO increases lead to higher ozone concentrations. Additionally, the meteorology of this episode shows that the ozone impacts elsewhere in the basin are not significant when DG is placed in Ventura. In Central Los Angeles the introduction of DG NO_x emissions has the effect of decreasing ozone concentrations locally and downwind. Central Los Angeles is a VOC-limited region, therefore increases in NO_x emissions decrease ozone concentrations. In fact, results show that the largest decreases in ozone

occur during the peak of the daylight cycle. Additionally, with the given meteorology, the placement of DG in Los Angeles county does not impact directly the ozone concentrations in the east side of the basin. The San Bernardino scenario predicts that ozone concentrations decrease locally, but increase downwind from the sources. This decrease is more pronounced during the nighttime, however, ozone increases up to $16\,ppb$ during the peaks of the daylight hours, especially after 12:00. The mixing of pollutants downwind and the large VOC-to-NO_x ratios leads to more ozone at higher NO_x emissions. Placement of DG in Riverside produces a similar behavior in ozone formation as in San Bernardino. Namely, local decreases during the night, downwind increases during the day. Although the decreases are similar in both counties, the increase in ozone concentration is markedly higher (up almost 50%) by placing DG in Riverside. One of the most prominent impacts are observed when DG is located near coastal areas such as Orange county. With the exception of the Ventura scenario, this represents the largest ozone increases from all scenarios explored. The positive and negative impacts have approximately the same magnitude, although they do not occur at the same time. As in the case of Riverside and San Bernardino, the largest decreases occur locally at nighttime just before sunrise at 7:00 am. The largest increases, downwind from sources, occur at around 16:00. Finally, the effects of placing DG in Orange county can be felt as far as the east side of Riverside.

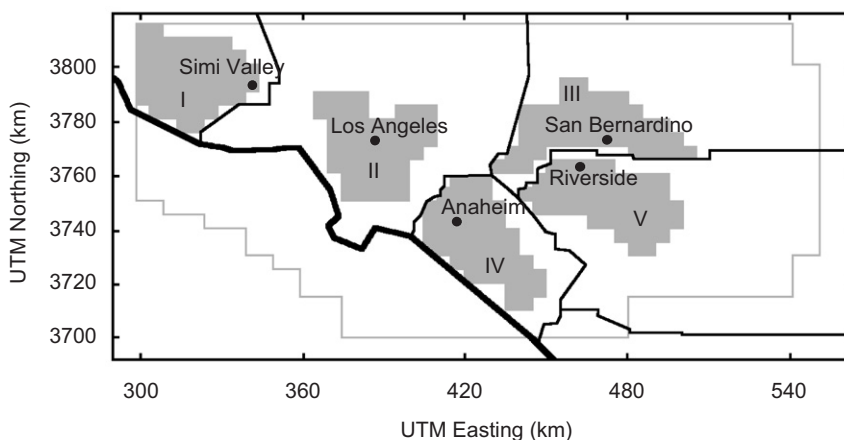Fig. 8 shows the 24-h average PM$_{2.5}$ aerosol concentrations impacts for each county scenario.

Fig. 6. Boundaries of the five regions in the SoCAB used to investigate the spatial sensitivity of DG emissions. Regions are located in Ventura (I), Los Angeles (II), San Bernardino (III), Orange (IV) and Riverside (V) counties.
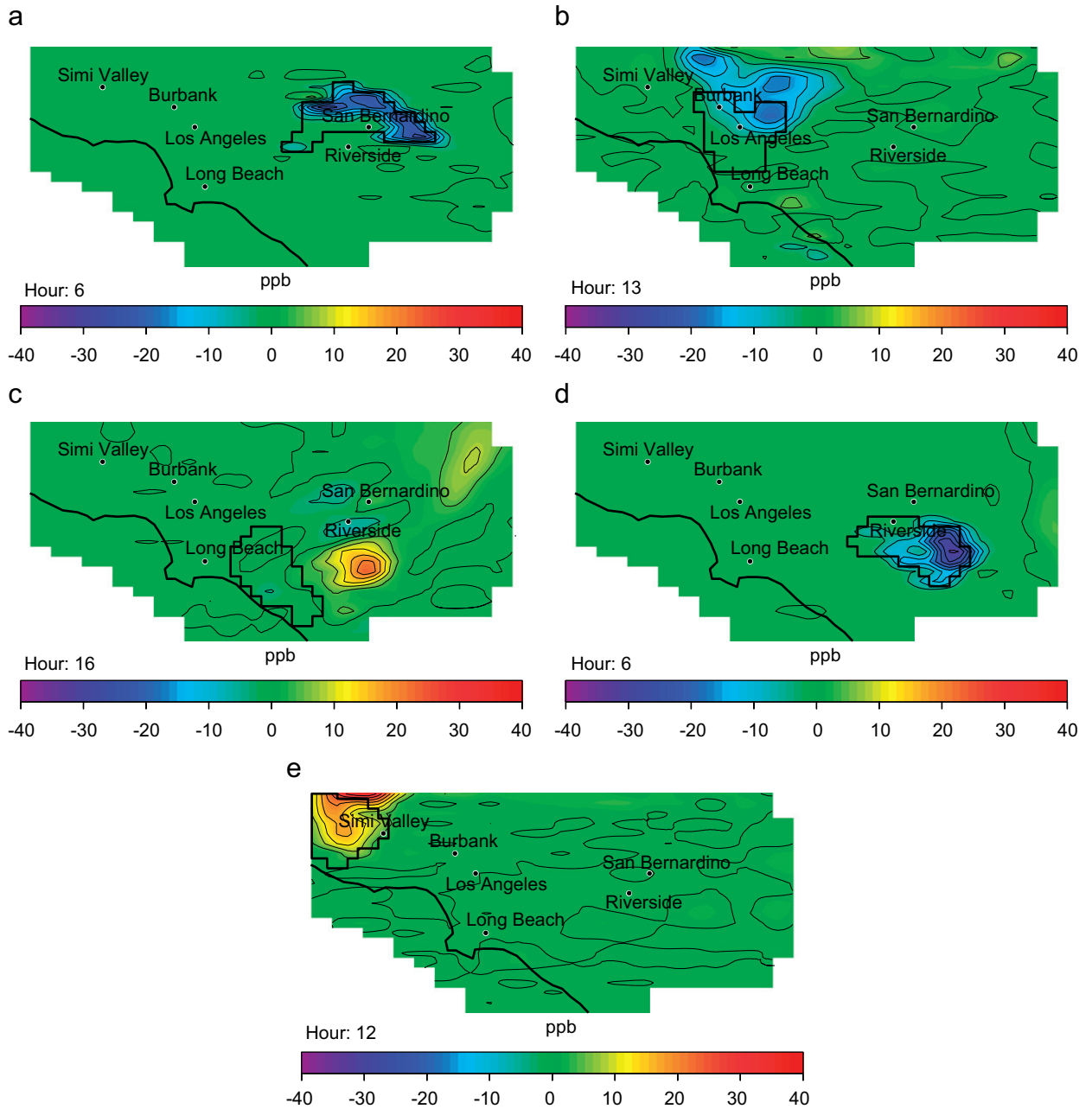
Fig. 7. Difference between spatial sensitivity scenarios and baseline ozone concentrations at the hour of maximum impact in different counties of the SoCAB. Boundaries of the DG emission sources are indicated for each scenario. Results are shown for (a) San Bernardino, (b) Los Angeles, (c) Orange, (d) Riverside, and (e) Ventura counties.

In general these impacts range from -2 to $14\,\mu g\,m^{-3}$. Also, the magnitude of positive impacts is larger than the magnitude of negative impacts, which implies that the influence of DG on $PM_{2.5}$ is to increase aerosol concentrations. With the exception of Central Los Angeles, all the other scenarios

produce impacts comparable to those observed in the high penetration scenario. Impacts on aerosol concentrations for the Los Angeles scenario shows increases of $PM_{2.5}$ concentrations north of the sources ($\pm 3\,\mu g\,m^{-3}$). The largest impacts occur for the Ventura scenario, since in the base-case no
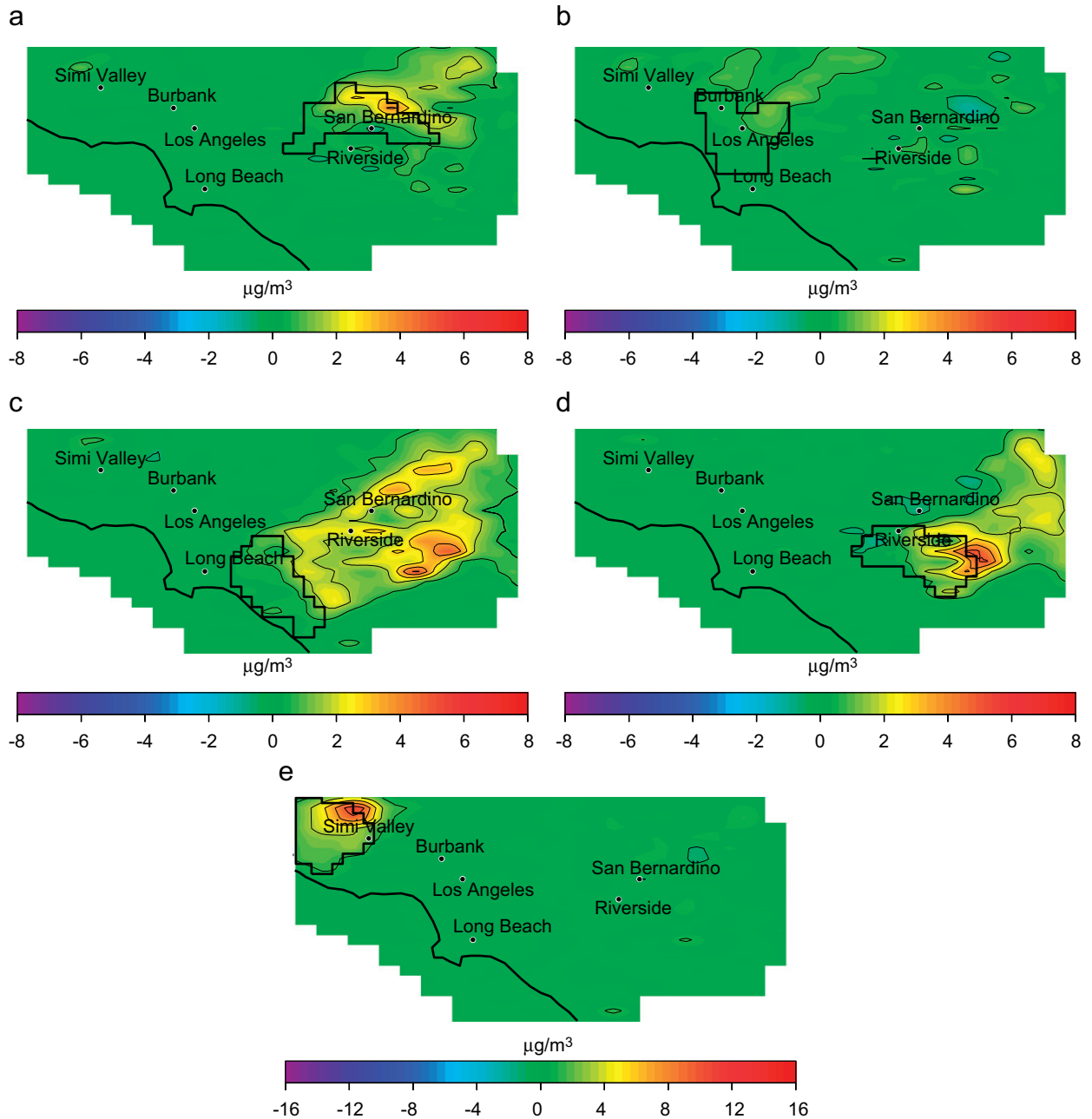
Fig. 8. Difference between spatial sensitivity scenarios and baseline 24-h average PM$_{2.5}$ aerosol concentrations in different counties of the SoCAB. Boundaries of the DG emission sources are indicated for each scenario. Results are shown for (a) San Bernardino, (b) Los Angeles, (c) Orange, (d) Riverside, and (e) Ventura counties.

major emissions are associated with this region. These impacts, however, are seen locally and indicate that DG installation in this region does not have an effect in other areas of the SoCAB. The effect of placing DG in both Riverside and San Bernardino is similar, namely those impacts do not

exceed 7.5 µg m^{-3}. Typically, high particulate matter concentrations are found in these regions. The contribution of additional DG, however, places additional concentrations locally but not downwind. The Orange county scenario puts most of the PM$_{2.5}$ impacts far from the sources, suggesting that

these aerosols are the result of gas to particle conversion from precursors. Therefore, the placement of DG in coastal areas shows to be of utmost importance for impacts in regions that already have high aerosol concentrations.

6. Conclusions

This study investigates the uncertainty and sensitivity of ozone and $PM_{2.5}$ aerosol to variations in selected input parameters using a Monte Carlo analysis. The selection of input parameters is based on their potential to affect the concentrations predicted by the model and also to reflect changes in emissions due to DG implementation in the SoCAB. Numerical simulations are performed with the CIT three-dimensional air quality model. Multiple model evaluations are completed, and statistical methods applied to identify those parameters with the largest effect on both the predicted concentrations of selected species and the uncertainty associated with their prediction.

This work provides the spatial and time-dependent variance associated with ozone and $PM_{2.5}$ concentrations predicted by the CIT three-dimensional air quality model. Results indicate that the variance of model concentrations is fully characterized with a normal probability density function both in space and time. Therefore, the domain-wide variance is reported adequately in terms of statistics such as the mean and standard deviation. The largest variance for ozone is approximately 42% (76 ± 32 ppb) whereas maximum concentrations show a variance of only 17% (221 ± 37 ppb). Sensitivity analyses demonstrate that the side boundary conditions of VOC and NO_x emissions are the major contributors to the ozone uncertainty in most regions throughout the SoCAB. Ozone boundary conditions have a marginal contribution to uncertainty in most locations, except for sites located near the boundaries of the computational domain.

For $PM_{2.5}$, the largest variance is $\sim$17% (48 ± 8 µg m^{-3}), but the largest domain-wide concentrations (108 ± 11 µg m^{-3}) have a variance of only 10%. Also, changes of 70–80% the nominal values of the selected input variables result in ozone and $PM_{2.5}$ concentration variability of 18–40%. Sensitivity analyses also show that in $PM_{2.5}$ is most sensitive to changes in NH_3 and NO_x emissions. Characterization of the influence of emissions is important since the implementation of DG has the

potential to introduce an important portion of emissions such as NO_x.

The effect of placing DG in specific regions of the SoCAB is explored with a spatial sensitivity analysis. The main conclusions of this study are:

- DG emissions applied in specific regions lead to a very complex spatially and time-dependent pollutant dynamics. Namely, ozone concentrations decrease locally, but increase downwind from the regional DG emission sources. The decrease is more pronounced during the nighttime, but during the daylight hours, when peak concentrations are observed, ozone increases. The mixing of pollutants downwind and the large VOC-to-NO_x ratios leads to more ozone for cases with higher NO_x emissions.

- Important spatial impacts are observed depending on the placement of DG emissions. For instance, the largest impacts for both ozone and $PM_{2.5}$ occur in areas where anthropogenic NO_x emissions are typically low, such as Ventura county. Also, when DG emissions are located near coastal areas, such as Orange county, they produce the largest ozone increases of all the scenarios explored. Furthermore, the Orange county scenario puts most of the $PM_{2.5}$ impacts far from the sources in regions with high aerosol concentrations, such as Riverside County. This observation implies that the additional aerosol is the product of gas to aerosol conversion from gas-phase precursors. These results suggest that placement of DG in coastal areas is of utmost importance to downstream regions that already have high aerosol concentrations.

- The magnitude of the largest impacts estimated in this study are greater and well beyond the contribution of emissions uncertainty to the estimated air quality model error.

- The analyses also suggest that the current model is sensitive enough to predict air quality impacts of DG emissions as long as changes in ozone are greater than 5 ppb and changes in $PM_{2.5}$ greater than 13 µg m^{-3}.

- In general, ozone impacts are higher than those of the highest DG penetration scenarios investigated by Rodriguez et al. (2006). Accumulation of mass emissions due to DG in one county leads to larger impacts than the same amount of emissions spread over a larger area such as the entire basin. For $PM_{2.5}$, with the exception of Central Los Angeles, all the other scenarios

produce impacts comparable to those observed in a high DG penetration scenario.

In summary, emissions introduced by DG implementation produce a highly non-linear response in time and space on pollutant concentrations. Results show that concentrating DG emissions in space or time will produce the largest air quality impacts in the SoCAB. Thus, in addition to the total amount of possible distributed generation to be installed, regulators should also consider the type of DG installed and their spatial distribution to avoid undesirable air quality impacts.

Acknowledgments

References

Bergin, M.S., Noblet, G.S., Petrini, K., Dhieux, J.R., Milford, J.B., Harley, R.A., 1999. Formal uncertainty analysis of a Lagrangian photochemical air pollution model. Environmental Science and Technology 33, 1116–1126.

CARB, 2002. The 2002 California Almanac of Emissions and Air Quality of the California Air Resources Board. ⟨http://www.arb.ca.gov/aqd/almanac/almanac.htm⟩.

CARB, 2003. Monitoring Sites in the South Coast Air Basin. California Air Resources Board web site. ⟨http://www.arb.ca.gov/adam/mapfiles/scozone.html⟩.

Derwent, R., Hov, Ø., 1988. Application of sensitivity and uncertainty analysis techniques to a photochemical ozone model. Journal of Geophysical Research 93, 5185–5199.

Gao, D., Stockwell, W.R., Milford, J.B., 1996. Global uncertainty analysis of a regional-scale gas-phase chemical mechanism. Journal of Geophysical Research 101, 9107–9119.

Gipson, G.L., Freas, W., Kelly, R., Meyer, E., 1981. Guideline for use of city-specific EKMA in preparing ozone SIPs. EPA-450/4-80-027, U.S. Environmental Protection Agency, Research Triangle Park, NC.

Grenfell, J.L., Savage, N.H., Harrison, R.M., Penkett, S.A., Forberich, O., Comes, F.J., Clemitshaw, K.C., Burgess, R.A., Cardenas, L.M., Davison, B., McFadyen, G.G., 1999. Tropospheric box-modelling and analytical studies of the hydroxyl (OH) radical and related species: comparison with observations. Journal of Atmospheric Chemistry 33, 183–214.

Griffin, R.J., Dabdub, D., Seinfeld, J.H., 2002a. Secondary organic aerosol 1. Atmospheric chemical mechanism for production of molecular constituents. Journal of Geophysical Research 107 (D17), 4332.

Griffin, R.J., Dabdub, D., Kleeman, M.J., Fraser, M.P., Cass, G.R., Seinfeld, J.H., 2002b. Secondary organic aerosol 3. Urban/regional scale model of size- and composition-resolved aerosols. Journal of Geophysical Research 107 (D17), 4334.

Griffin, R.J., Nguyen, K., Dabdub, D., 2003. A coupled Hydrophobic-Hydrophilic model for predicting secondary organic aerosol formation. Journal of Atmospheric Chemistry 44, 171–190.

Hakami, A., Odman, M.T., Russell, A.G., 2003. High-order, direct sensitivity analysis of multidimensional air quality models. Environmental Science and Technology 37, 2442–2452.

Hanna, S.R., Davis, J.M., 2002. Evaluation of a photochemical grid model using estimates of concentration probability density functions. Atmospheric Environment 36, 1793–1798.

Hanna, S.R., Chang, J.C., Fernau, M., 1998. Monte Carlo estimates of uncertainties in predictions by a photochemical grid model (UAM-IV) due to uncertainties in input variables. Atmospheric Environment 32, 3619–3628.

Hanna, S.R., Lu, Z.G., Frey, H.C., Wheeler, N., Vukovich, J., Arunachalam, S., Fernau, M., Hansen, D.A., 2001. Uncertainties in predicted ozone concentrations due to input uncertainties for the UAM-V photochemical grid model applied to the July 1995 OTAG domain. Atmospheric Environment 35, 891–903.

Helton, J.C., 1993. Uncertainty and sensitivity analysis techniques for use in performance assessment for radioactive waste disposal. Reliability Engineering and System Safety 42, 327–367.

Iman, R.L., Conover, W.J., 1980. Small sample sensitivity analysis techniques for computer models with an application to risk assessment. Communications in Statistics A9, 1749–1842.

McCay, M.D., Conover, W.J., Beckman, R.J., 1979. A comparison of three methods for selecting values of input variables in the analysis of output from a computer code. Technometrics 221, 239–245.

Meng, Z., Dabdub, D., Seinfeld, J.H., 1997. Chemical coupling between atmospheric ozone and particulate matter. Science 277, 116–119.

Meng, Z., Dabdub, D., Seinfeld, J.H., 1998. Size-resolved and chemically resolved model of atmospheric aerosol dynamics. Journal of Geophysical Research 103, 3419–3435.

Meyer, E.L., 1986. Review of control strategies for ozone and their effects on other environmental issues. EPA-450/4-85-0011, U.S. Environmental Protection Agency, Research Triangle Park, NC.

Moore, G.E., Londergan, R.J., 2001. Sampled Monte Carlo uncertainty analysis for photochemical grid models. Atmospheric Environment 35, 4863–4876.

Nguyen, K., Dabdub, D., 2002. NO_x and VOC control and its effects on the formation of aerosols. Aerosol Science and Technology 36, 560–572.

Owen, A.B., 1992. A central limit theorem for Latin hypercube sampling. Journal of the Royal Statistical Society Series B 54, 541–551.

Phenix, B.D., Dinaro, J.L., Tatang, M.A., Tester, J.W., Howard, J.B., McRae, G.J., 1998. Incorporation of parametric uncertainty into complex kinetic mechanisms: application to hydrogen oxidation in supercritical water. Combustion and Flame 112, 132–146.

Pun, B.K., Griffin, R.J., Seigneur, C., Seinfeld, J.H., 2002. Secondary organic aerosol 2. Thermodynamic model for gas/particle partitioning of molecular constituents. Journal of Geophysical Research 107 (D17), 4333.

Rodriguez, M.A., Dabdub, D., 2003. Monte Carlo uncertainty and sensitivity analysis of the CACM chemical mechanism. Journal of Geophysical Research 108 (D15), 4443.

Rodriguez, M.A., Carreras-Sospedra, M., Medrano, M., Brouwer, J., Samuelsen, G.S., Dabdub, D., 2006. Air quality impacts of distributed power generation in the South Coast Air Basin of California 1: scenario development and modeling analysis. Atmospheric Environment 40, 5508–5521.

Russell, A.G., Dennis, R., 2000. NARSTO critical review of photochemical models and modeling. Atmospheric Environment 34, 2283–2324.

Sax, T., Isakov, V., 2003. A case study for assessing uncertainty in local-scale regulatory air quality modeling applications. Atmospheric Environment 37, 3481–3489.

Stein, M., 1987. Large sample properties of simulations using Latin hypercube sampling. Technometrics 29, 143–151.

Vardoulakis, S., Fisher, B.E.A., Gonzalez-Flesca, N., Pericleous, K., 2002. Model sensitivity and uncertainty analysis using roadside air quality measurements. Atmospheric Environment 36, 2121–2134.

Vuilleumier, L., Bamer, J.T., Harley, R.A., Brown, N.J., 2001. Evaluation of nitrogen dioxide photolysis rates in an urban area using data from the 1997 Southern California Ozone Study. Atmospheric Environment 35, 6525–6537.

Yang, Y.J., Wilkinson, J.G., Russell, A.G., 1997. Fast, direct sensitivity analysis of multidimensional models. Environmental Science and Technology 31, 2859–2868.